CONFIDENTIAL

Copy
RM E9I22a

NACA RM E9I22a

NACA

RESEARCH MEMORANDUM

EXPERIMENTAL PRESSURE DISTRIBUTIONS OVER WING TIPS AT MACH NUMBER 1.9

II - WING TIP WITH SUBSONIC TRAILING EDGE

By Harold Mirels and James M. Jagger

Lewis Flight Propulsion Laboratory
Cleveland, Ohio

NATIONAL ADVISORY COMMITTEE
FOR AERONAUTICS

WASHINGTON
December 21, 1949

CONFIDENTIAL

NATIONAL ADVISORY COMMITTEE FOR AERONAUTICS

RESEARCH MEMORANDUM

EXPERIMENTAL PRESSURE DISTRIBUTIONS OVER WING TIPS AT MACH NUMBER 1.9

II - WING TIP WITH SUBSONIC TRAILING EDGE

By Harold Mirels and James M. Jagger

SUMMARY

An investigation has been conducted at a Mach number of 1.90 to determine the experimental pressure distribution over a wing tip in the region influenced by a sharp subsonic trailing edge. The wing section was a symmetrical wedge of 5° 43' total included angle in the free-stream direction. The investigation was conducted over a range of angles of attack from -10° to 10° at a Reynolds number of 3.4×10^{6} per foot.

The experimental pressure distribution in the region influenced by the subsonic trailing edge was generally in poor agreement with linearized theory. The difference between theory and experiment was attributed to separation associated with the adverse pressure gradient predicted by linearized theory for this region.

INTRODUCTION

A variety of methods based on linearized theory are available for determining the pressure distribution over thin three-dimensional wings in supersonic flight (for example, references 1 to 5). The pressure distributions predicted by linearized theory have been found to be fairly reliable for thin wings at small angles of attack, except for certain types of wing region. In particular, experimental pressure distributions reported in references 6 and 7 indicate that the agreement between linearized theory and experiment is poor for wing regions influenced by a subsonic trailing edge. The wing model investigated in references 6 and 7 was a swept wing of biconvex section 7 percent thick in the streamwise direction. Additional investigations of airfoils composed of thinner sections and different thickness distributions appear desirable to evaluate the validity of linear theory near a subsonic trailing edge.

An investigation was undertaken at the NACA Lewis laboratory to determine pressure distributions (on wings having wedge sections 5 percent thick in streamwise direction) in regions where the assumption of linearized theory may be invalid. The first part of this investigation (reference 8) concerned experimental pressures in a wing region influenced by a sharp subsonic leading edge. Local expansions, beyond the values predicted by linearized theory, were found to occur on the top surface nearest the subsonic edge. Results of the second part of this investigation are presented herein. Experimental pressures in the neighborhood of a sharp subsonic trailing edge are compared with linearized theory.

APPARATUS

The investigation was conducted in the Lewis 18- by 18-inch supersonic tunnel. The Mach number in the region of the wing was 1.90 ±0.01. The Reynolds number was 3.4×10^6 per foot. A photograph of the wing installed in the tunnel is shown in figure 1. The angle of attack could be read to an accuracy of ±2.5 minutes.

A sketch of the wing showing the principal dimensions and the location of the static-pressure orifices is shown in figure 2. The wing profile section, in the free-stream direction, was a symmetrical wedge of 5° 43' total included angle (that is, thickness ratio of 5 percent). The leading edge was swept at 30°, the maximum thickness line (from the tip) at 55° 37', and the subsonic trailing edge at 73° 43'. The orifices were 0.010 inch in diameter, sharp-edged, and free of burs.

The wing model was machined from two pieces of tool steel. After installation of the pressure tubes, the two pieces of the wing were fastened together and the entire model was finish-ground. The plan-form edges were ground to knife edges.

SYMBOLS

The following symbols are used in this report:

C_p pressure coefficient, $\Delta p/q$

M Mach number

m slope (y/x) of plan-form edge or maximum thickness line

Δp difference between local wing pressure and free-stream static pressure

q free-stream dynamic pressure, $\frac{1}{2}\rho V^2$

V free-stream velocity

x,y,z Cartesian coordinate system

α angle of attack

β cotangent of Mach angle, $\sqrt{M^2-1}$

τ wedge half-angle measured in free-stream direction

ρ free-stream density

Subscripts:

B bottom surface of wing

T top surface of wing

1 plan-form leading edge

2 maximum thickness line

3 plan-form trailing edge

THEORY

The pressure coefficient on the wing at angle of attack α can be expressed, according to linearized theory, as

$$C_p = C_p(\tau) + C_p(\alpha) \tag{1}$$

where

$C_p(\tau)$ pressure coefficient on surface of wing at zero angle of attack

$C_p(\alpha)$ pressure coefficient on surface of flat plate of same plan form at angle of attack α

By the methods of reference 1 or 4, the pressure coefficient $C_p(\tau)$ for the portion of the wing model upstream of the midchord can be expressed as follows:

For $\frac{\beta y}{x} < -1.11$,

$$C_p(\tau) = \frac{2\tau}{\beta\sqrt{1 - \frac{1}{(\beta m_1)^2}}} \tag{2a}$$

For $-1.11 < \frac{\beta y}{x} \leqq -1.00$,

$$C_p(\tau) = \frac{2\tau}{\beta}\left[\frac{1}{\sqrt{1 - \frac{1}{(\beta m_1)^2}}} - \frac{2}{\sqrt{1 - \frac{1}{(\beta m_2)^2}}}\right] \tag{2b}$$

For $-1.00 \leqq \frac{\beta y}{x} \leqq -0.47$,

$$C_p(\tau) = \frac{2\tau}{\beta\pi}\left\{\frac{1}{\sqrt{1 - \frac{1}{(\beta m_1)^2}}}\left[\frac{\pi}{2} + \sin^{-1}\left(\frac{\frac{\beta^2 m_1 y}{x} - 1}{\frac{\beta y}{x} - \beta m_1}\right)\right] - \right.$$

$$\frac{2}{\sqrt{1 - \frac{1}{(\beta m_2)^2}}}\left[\frac{\pi}{2} + \sin^{-1}\left(\frac{\frac{\beta^2 m_2 y}{x} - 1}{\frac{\beta y}{x} - \beta m_2}\right)\right] +$$

$$\left.\frac{1}{\sqrt{\frac{1}{(\beta m_3)^2} - 1}} \log_e \frac{\frac{\beta^2 m_3 y}{x} - 1 - \sqrt{\left[1 - \left(\frac{\beta y}{x}\right)^2\right]\left(1 - \beta^2 m_3{}^2\right)}}{\frac{\beta y}{x} - \beta m_3}\right\} \tag{2c}$$

The coordinate system is illustrated in figure 2. The slopes m_1, m_2, and m_3 refer to the slopes of the leading edge, the maximum thickness line (from the tip), and the trailing edge, respectively. For the wing investigated, these slopes are 1.732, -0.684, and -0.292, respectively. The wedge half-angle τ is 0.050 radian.

The pressure coefficients on the flat plate at angle of attack, obtained from equation (12) of reference 5, are given by

$$C_{p,T}(\alpha) = -\frac{2\alpha}{\beta\pi}\frac{(1+k_1)}{\sqrt{k_1}}\tan^{-1}\sqrt{\frac{k_1\left[k_3\left(1-\frac{\beta y}{x}\right)-1-\frac{\beta y}{x}\right]}{(k_3+k_1)\left(1+\frac{\beta y}{x}\right)}} \tag{3}$$

and

$$C_{p,T}(\alpha) = -C_{p,B}(\alpha) \tag{4}$$

where

$$k_1 = \frac{\beta m_1+1}{\beta m_1-1} \quad \text{and} \quad k_3 = \frac{\beta m_3+1}{1-\beta m_3}$$

Equation (3) assumes that the Kutta-Joukowski condition applies at the trailing edge.

RESULTS AND DISCUSSION

The wing was investigated at angles of attack from -10° to 10°. Because the wing is symmetrical, the pressures on one surface at a positive angle of attack should equal the pressures on the opposite surface at the same negative angle of attack. Experimental data for both positive and negative angles of attack have therefore been reduced in figures 3 and 4 to correspond to the top and bottom surfaces of the wing through the positive angle-of-attack range.

Pressures at each station. - The experimental variation of pressure coefficient with angle of attack at each spanwise station is compared with linearized theory in figure 3. Two distinct sets of data are presented for stations $\beta y/x$ = -1.50, -0.78, and -0.71 (figs. 3(a), 3(e), and 3(f)), because orifices were located on

both top and bottom surfaces of the wing for each of these stations. Differences between the two sets of data are probably due to deviations from the ideal conditions (model symmetry and uniform tunnel flow) assumed by the data-reduction technique.

At station $\beta y/x = -1.50$ (fig. 3(a)), linearized theory and experimental data are in good agreement at the small angles of attack, but continuously diverge with increasing angle of attack. A similar trend was observed in reference 8 for stations influenced only by a sharp supersonic leading edge.

The remaining stations (figs. 3(b) to 3(h)) are in the region of influence of both the maximum thickness line ($\beta y/x = -1.11$) and the subsonic trailing edge ($\beta y/x = -0.47$). The data at these stations exhibit no systematic divergence from theory with increasing angle of attack, such as that observed at station $\beta y/x = -1.50$. The experimental data can be best discussed from a consideration of the spanwise distribution of pressures at constant angle of attack. This discussion is presented in the next section.

Spanwise variation of pressures. - The spanwise variation of pressure coefficient at an angle of attack of 0° is compared with linearized theory in figure 4(a). Experimental pressures in the region influenced by the subsonic trailing edge show only a slight increase with $\beta y/x$ and are in sharp contrast with the predictions of linearized theory. The adverse pressure gradient predicted by linearized theory indicates that viscous effects will tend to become prominent in this region. The flatness of the pressure-distribution curve suggests that separation has occurred. This separation probably originated in the vicinity of the Mach line from the wing tip, because linearized theory indicates a steep compression on this line.

Experimental data for angles of attack of 3°, 6°, and 9° are shown in figures 4(b) to 4(d). The disagreement between linearized theory and experiment for the top surface of the wing is similar to that observed at zero angle of attack. With increasing angle of attack, the experimental pressures on the bottom surface of the wing appear to show better agreement with linearized theory. This apparent agreement may be associated with the more favorable pressure gradient.

CONCLUDING REMARKS

The experimental pressure distribution in the region influenced by the subsonic trailing edge is generally in poor agreement with linearized theory. The difference between theory and experiment is attributed to separation associated with the adverse pressure gradient predicted by linearized theory for this region. The lack of agreement in this region is qualitatively similar to the results of references 6 and 7.

Lewis Flight Propulsion Laboratory,
National Advisory Committee for Aeronautics,
Cleveland, Ohio.

REFERENCES

1. Jones, Robert T.: Thin Oblique Airfoils at Supersonic Speed. NACA Rep. 851, 1946.

2. Stewart, H. J.: The Lift of a Delta Wing at Supersonic Speeds. Quarterly Appl. Math., vol. IV, no. 3, Oct. 1946, pp. 246-254.

3. Brown, Clinton E.: Theoretical Lift and Drag of Thin Triangular Wings at Supersonic Speeds. NACA Rep. 839, 1946.

4. Evvard, John C.: Distribution of Wave Drag and Lift in the Vicinity of Wing Tips at Supersonic Speeds. NACA TN 1382, 1947.

5. Evvard, John C.: Theoretical Distribution of Lift on Thin Wings at Supersonic Speeds (An Extension). NACA TN 1585, 1948.

6. Frick, Charles W., and Boyd, John W.: Investigation at Supersonic Speed (M = 1.53) of the Pressure Distribution over a 63° Swept Airfoil of Biconvex Section at Zero Lift. NACA RM A8C22, 1948.

7. Boyd, John W., Katzen, Elliott D., Frick, Charles W.: Investigation at Supersonic Speed (M = 1.53) of the Pressure Distribution over a 63° Swept Airfoil of Biconvex Section at Angles of Attack. NACA RM A8F22, 1948.

8. Jagger, James M., and Mirels, Harold: Experimental Pressure Distributions over Wing Tips at Mach number 1.9. I - Wing Tip with Subsonic Leading Edge. NACA RM E8K26, 1949.

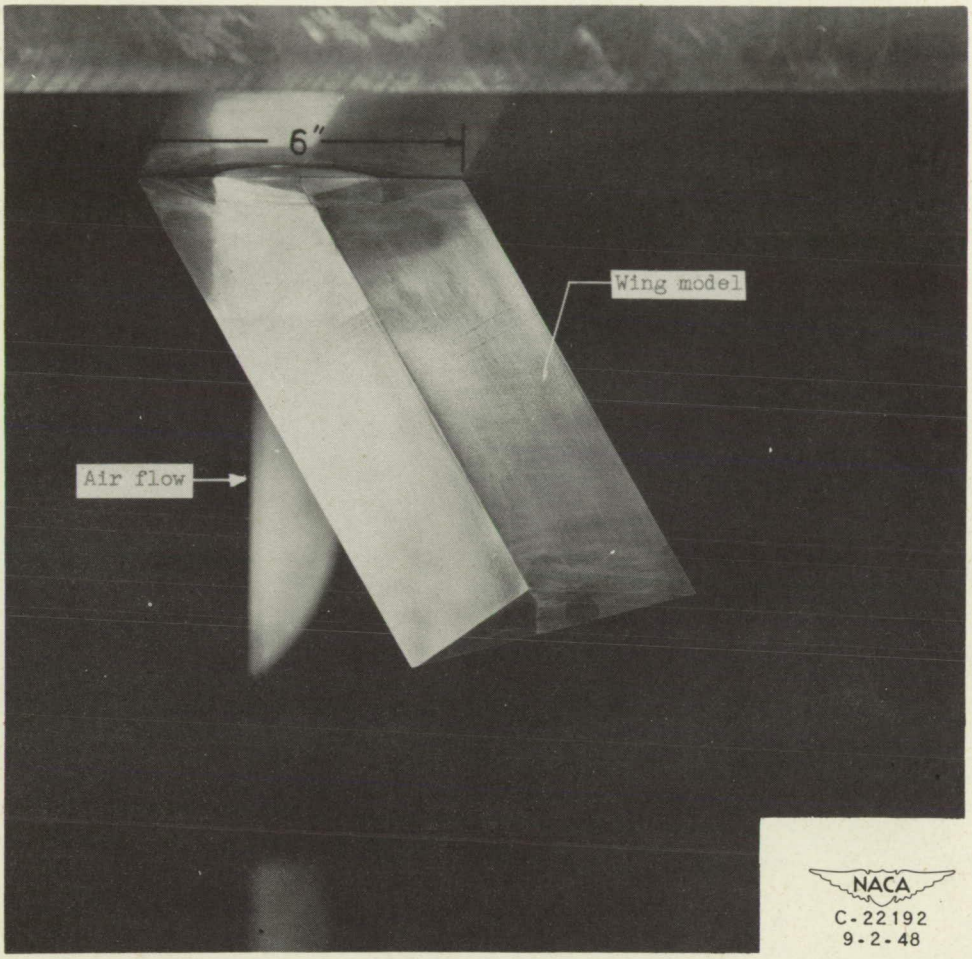

Figure 1. - Installation of wing-tip model in 18- by 18-inch supersonic tunnel.

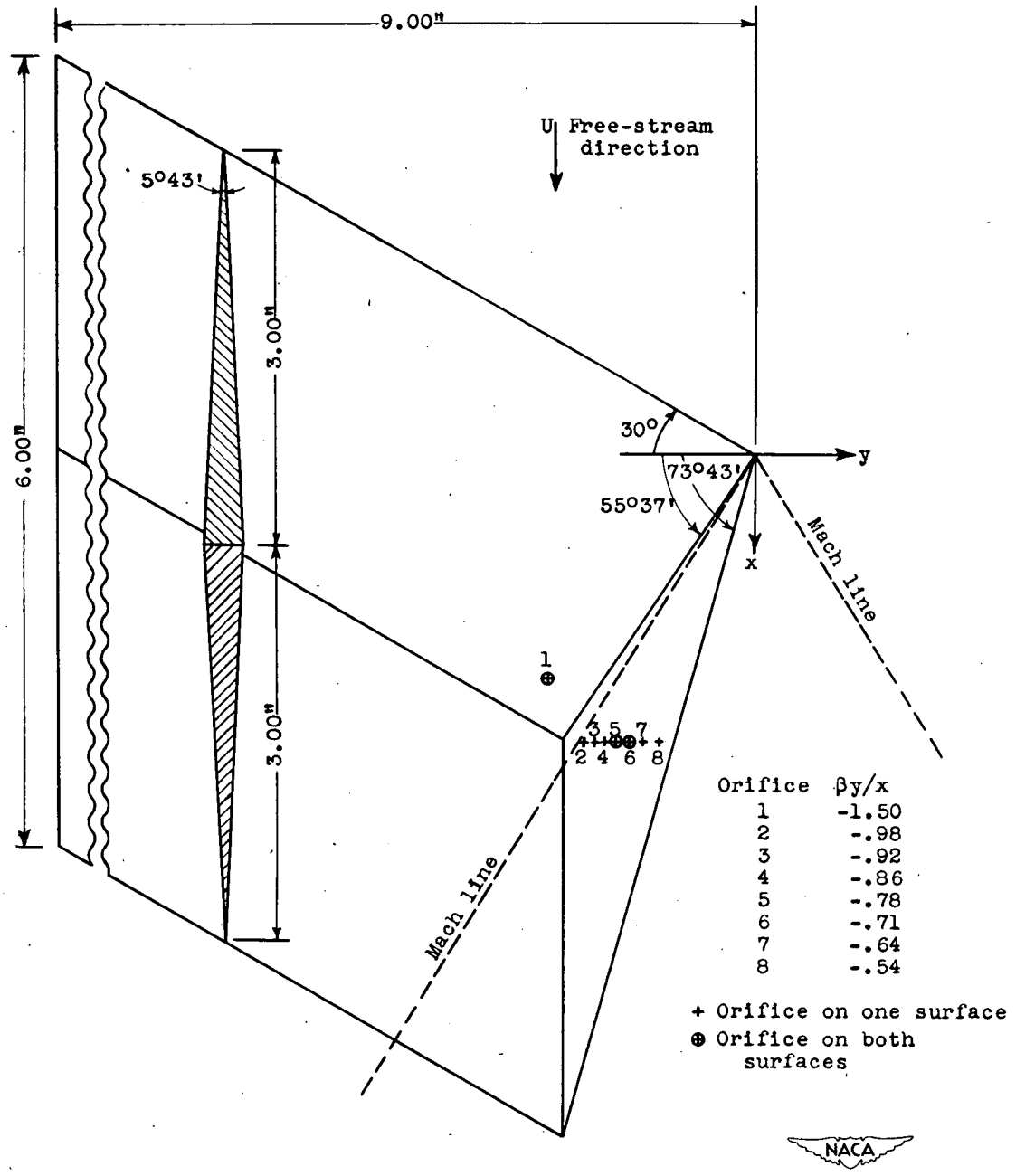

Figure 2. - Sketch of wing-tip model showing principal dimensions and locations of pressure orifices. All sections are symmetric double wedges of 5°43' included angle in free-stream direction.

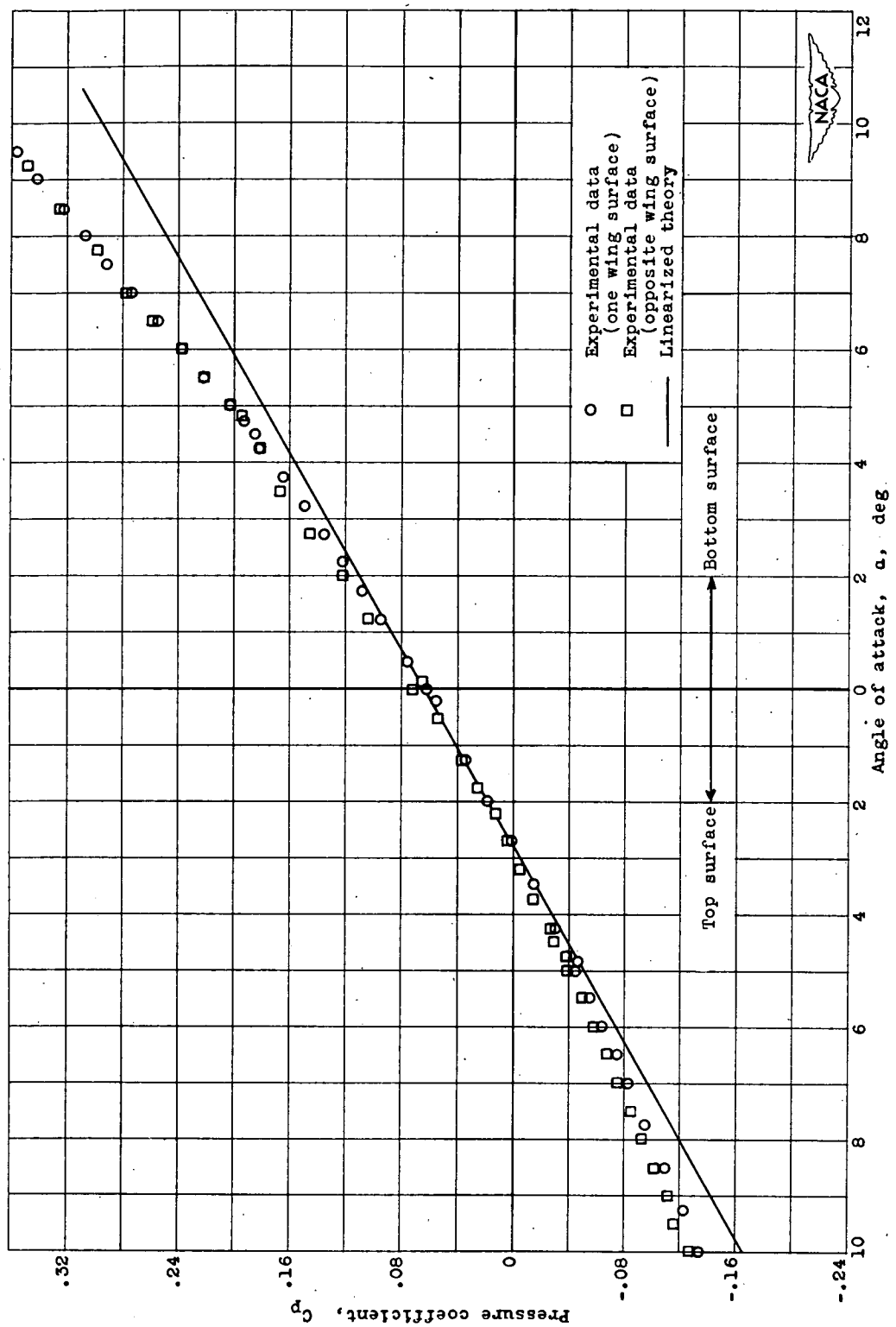

(a) $\beta y/x = -1.50$.

Figure 3. - Variation of pressure coefficient with angle of attack at each orifice station.

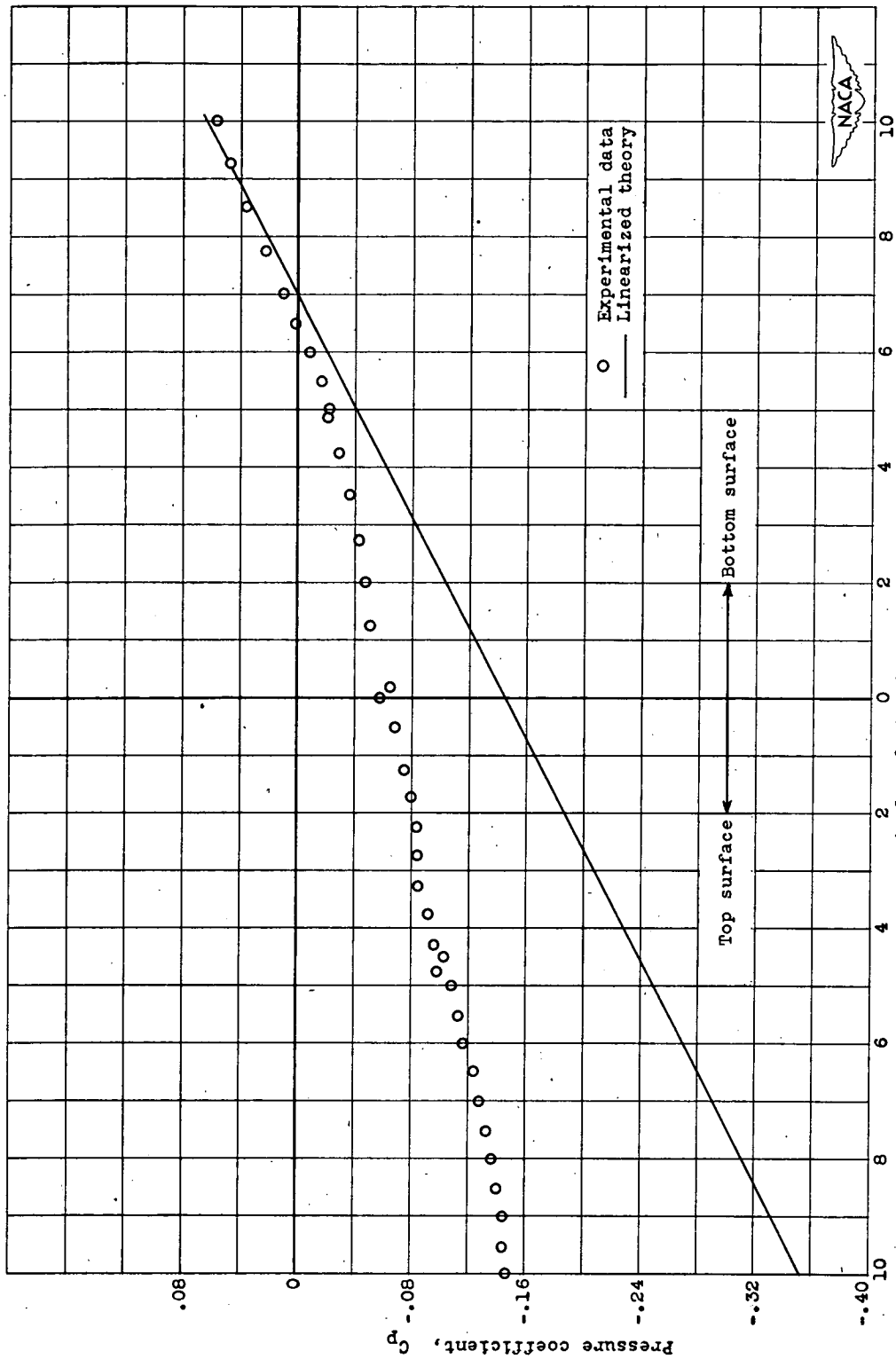

(b) $\beta y/x = -0.98$.

Figure 3. - Continued. Variation of pressure coefficient with angle of attack at each orifice station.

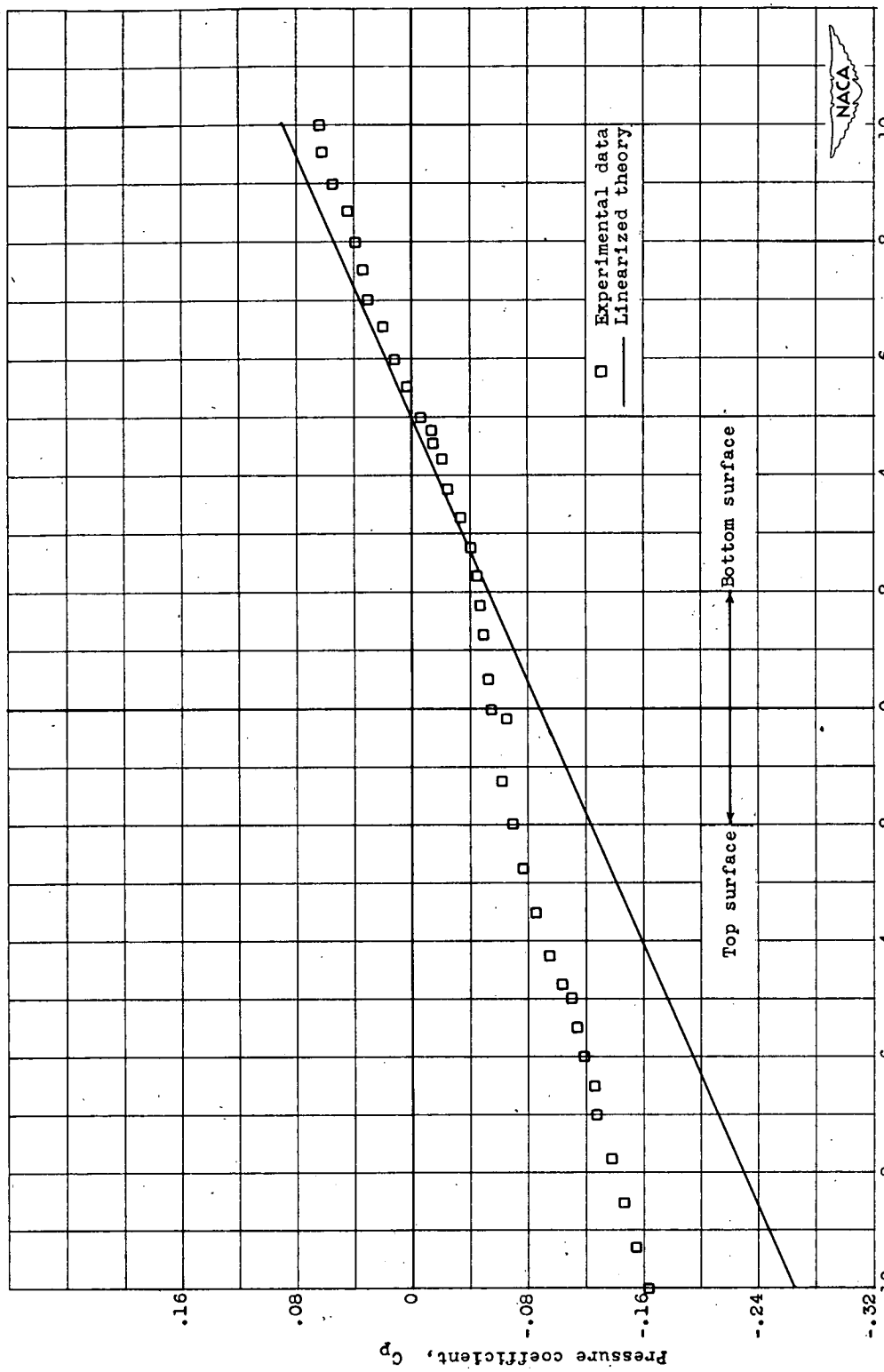

(c) $\beta y/x = -0.92$.

Figure 3. - Continued. Variation of pressure coefficient with angle of attack at each orifice station.

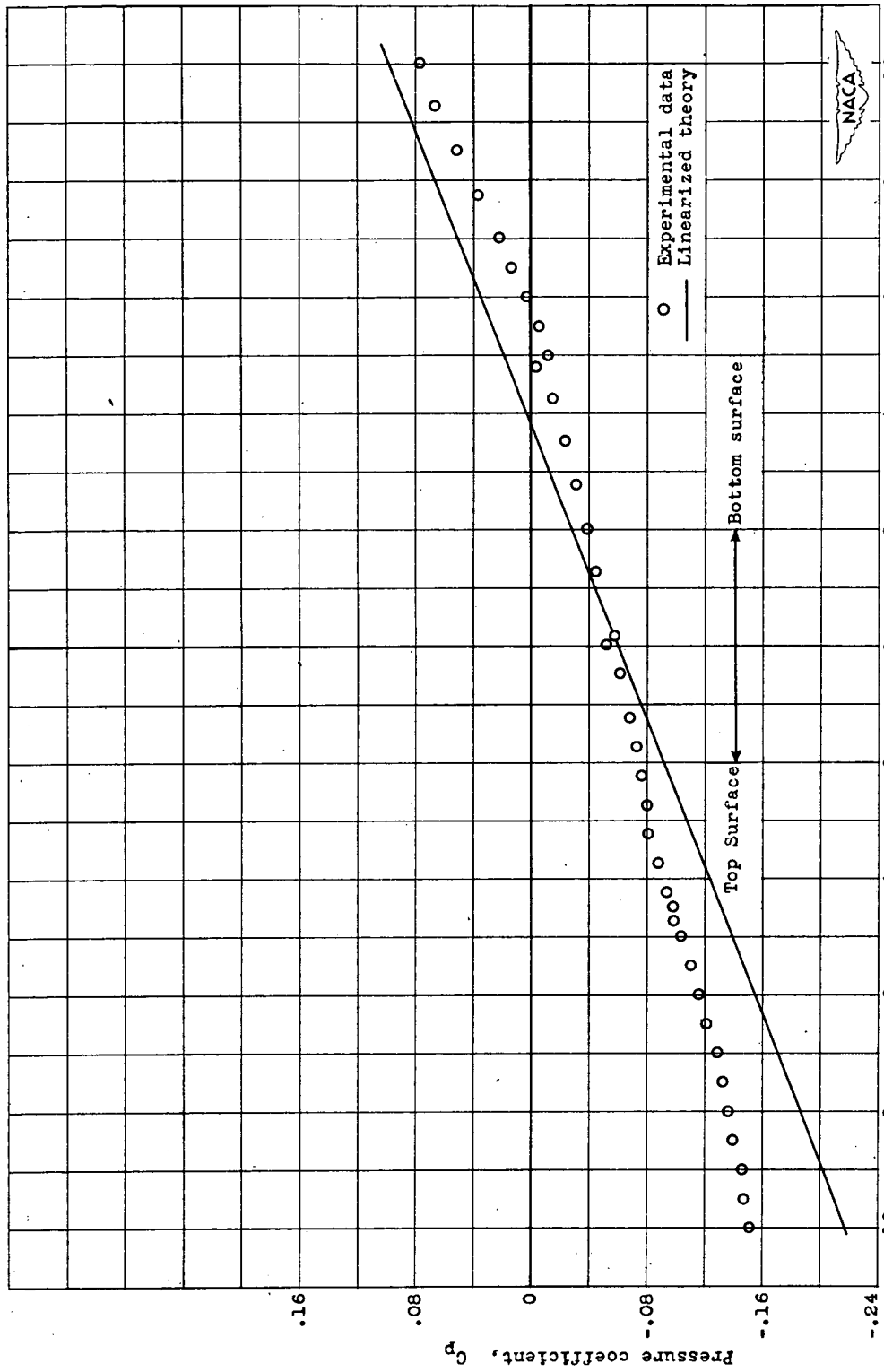

(d) $\beta y/x = -0.86$.

Figure 3. - Continued. Variation of pressure coefficient with angle of attack at each orifice station.

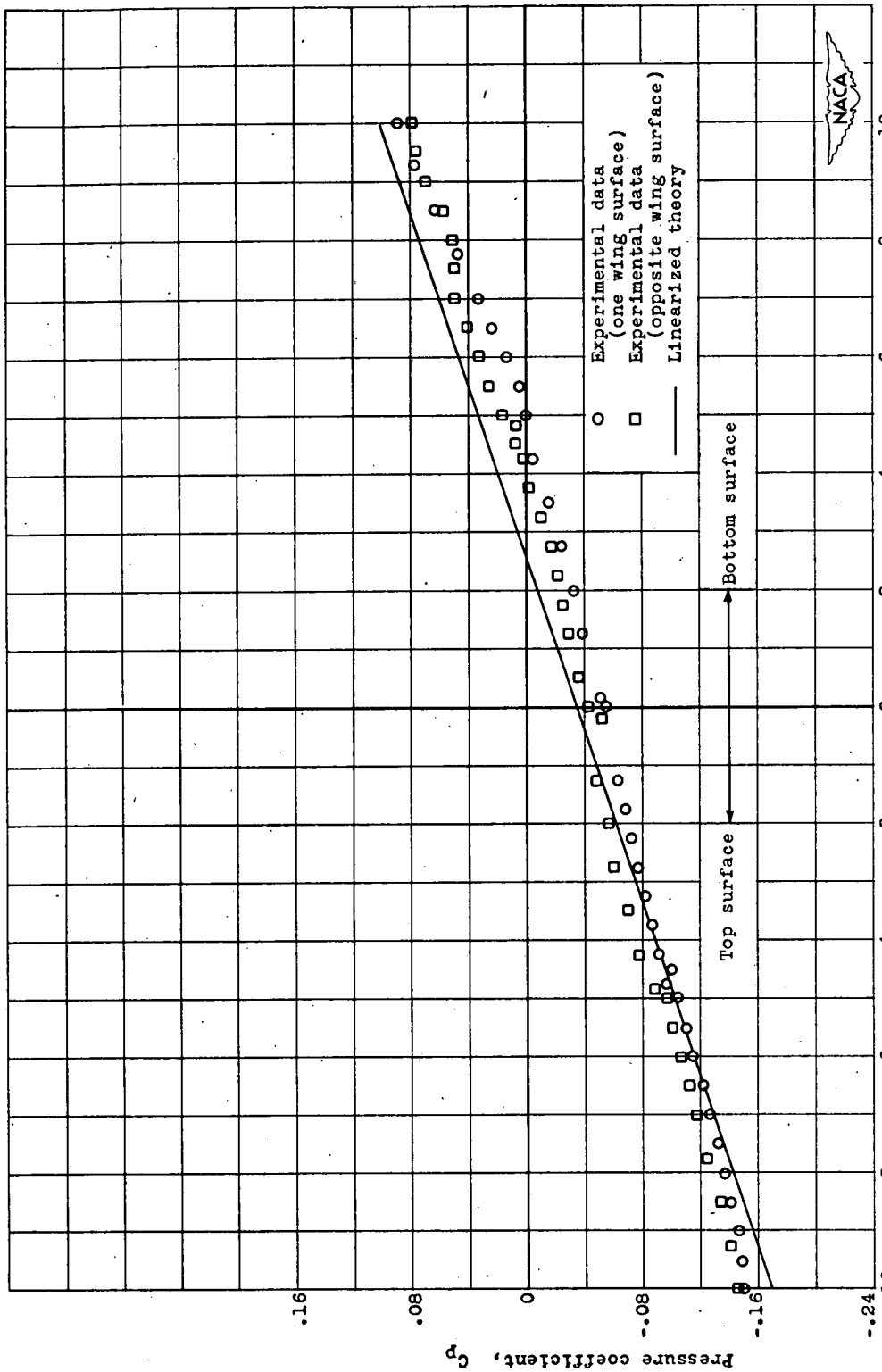

(e) $\beta y/x = -0.78$.

Figure 3. - Continued. Variation of pressure coefficient with angle of attack at each orifice station.

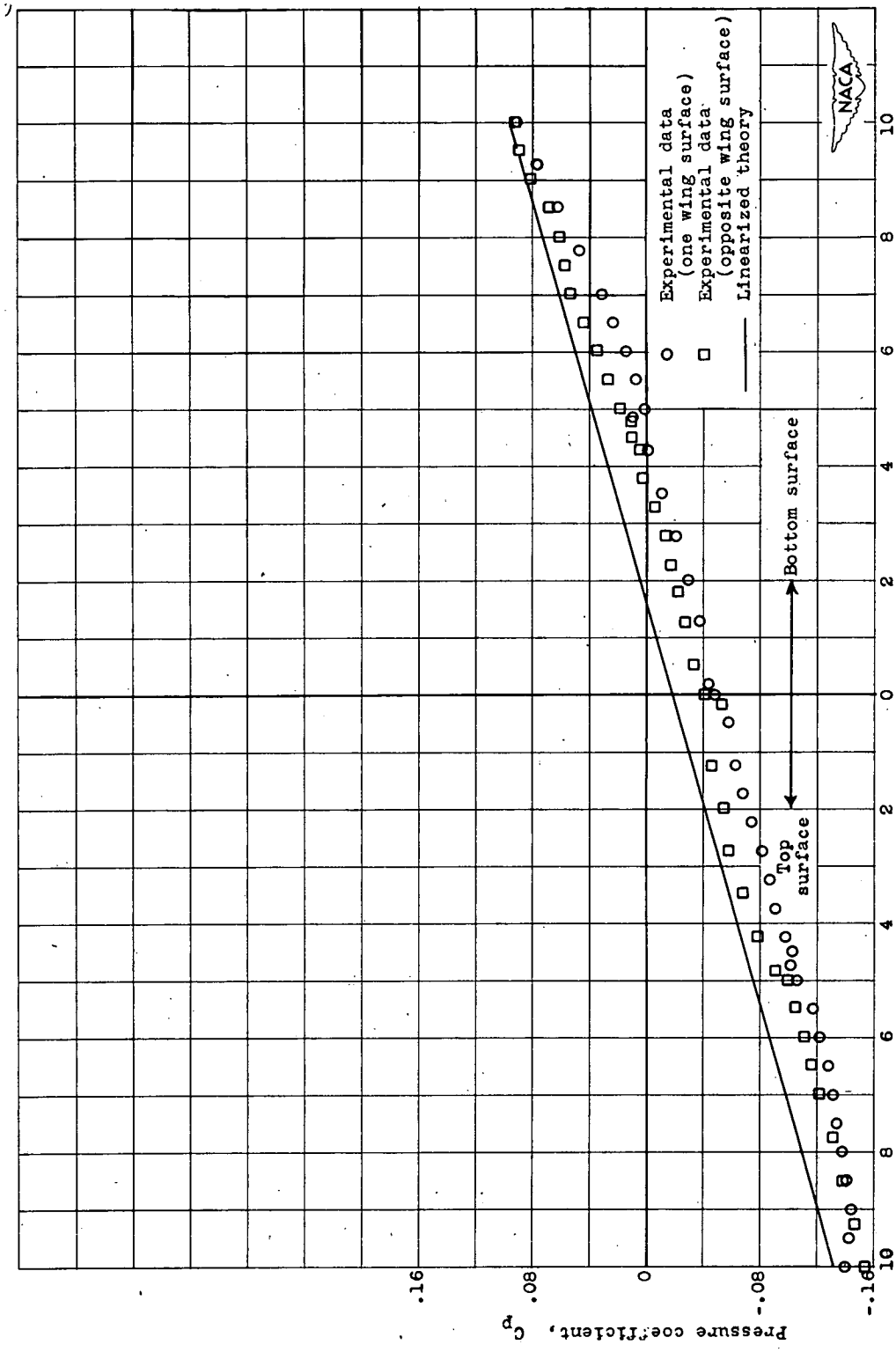

(f) $\beta y/x = -0.71$.

Figure 3. - Continued. Variation of pressure coefficient with angle of attack at each orifice station.

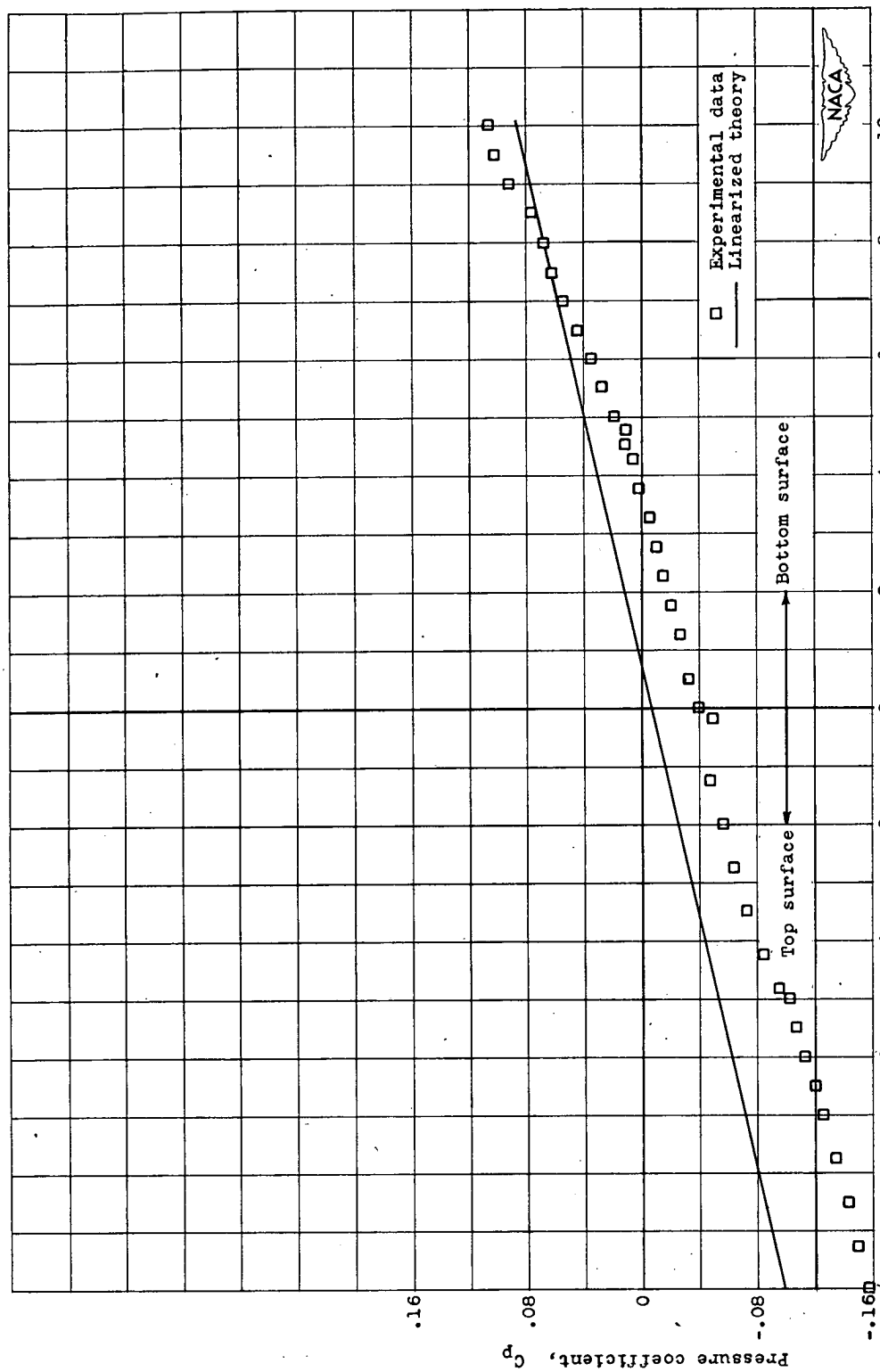

(g) $\beta y/x = -0.64$.

Figure 3. - Continued. Variation of pressure coefficient with angle of attack at each orifice station.

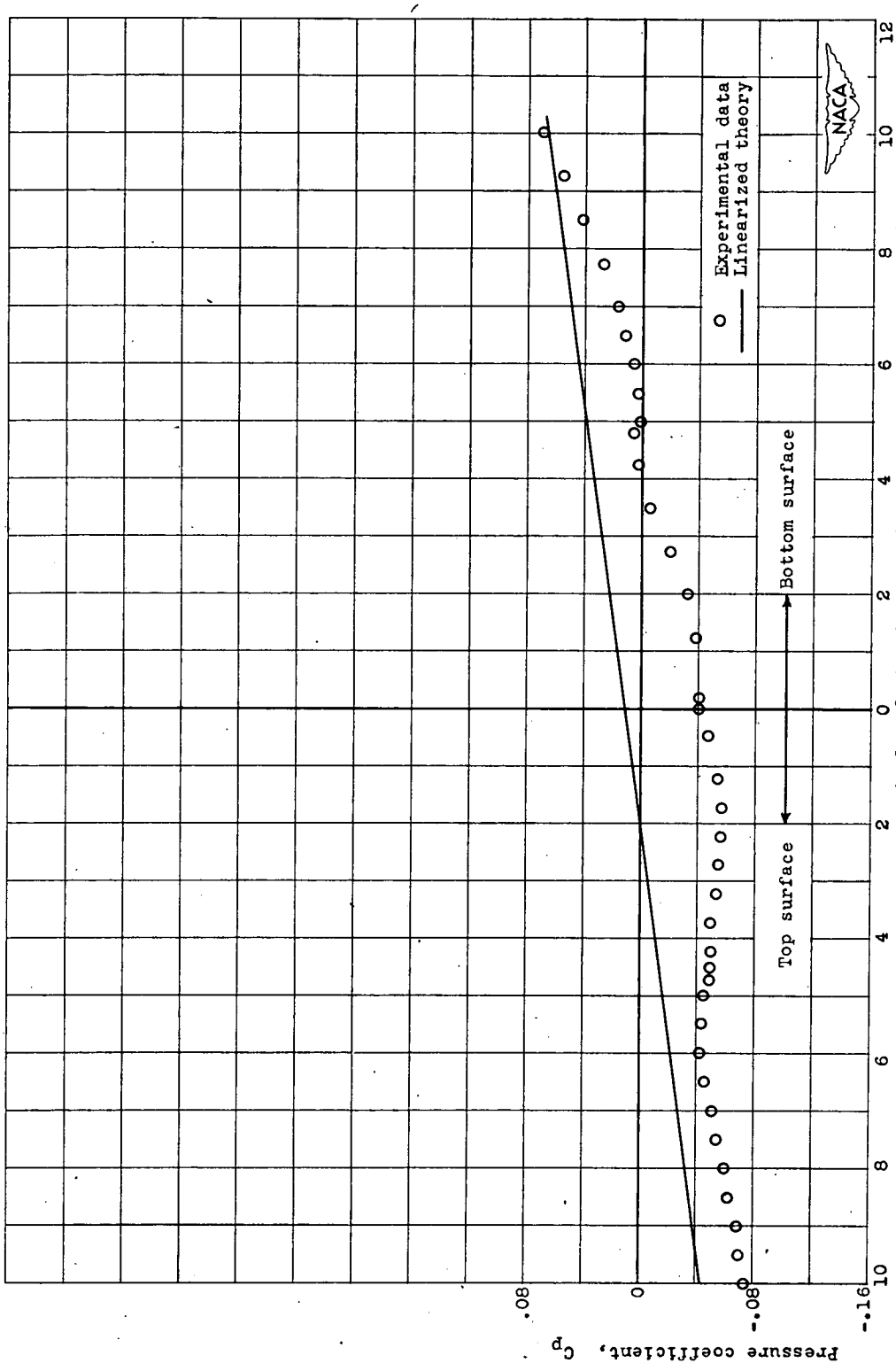

(h) $\beta y/x = -0.54$.

Figure 3. - Concluded. Variation of pressure coefficient with angle of attack at each orifice station.

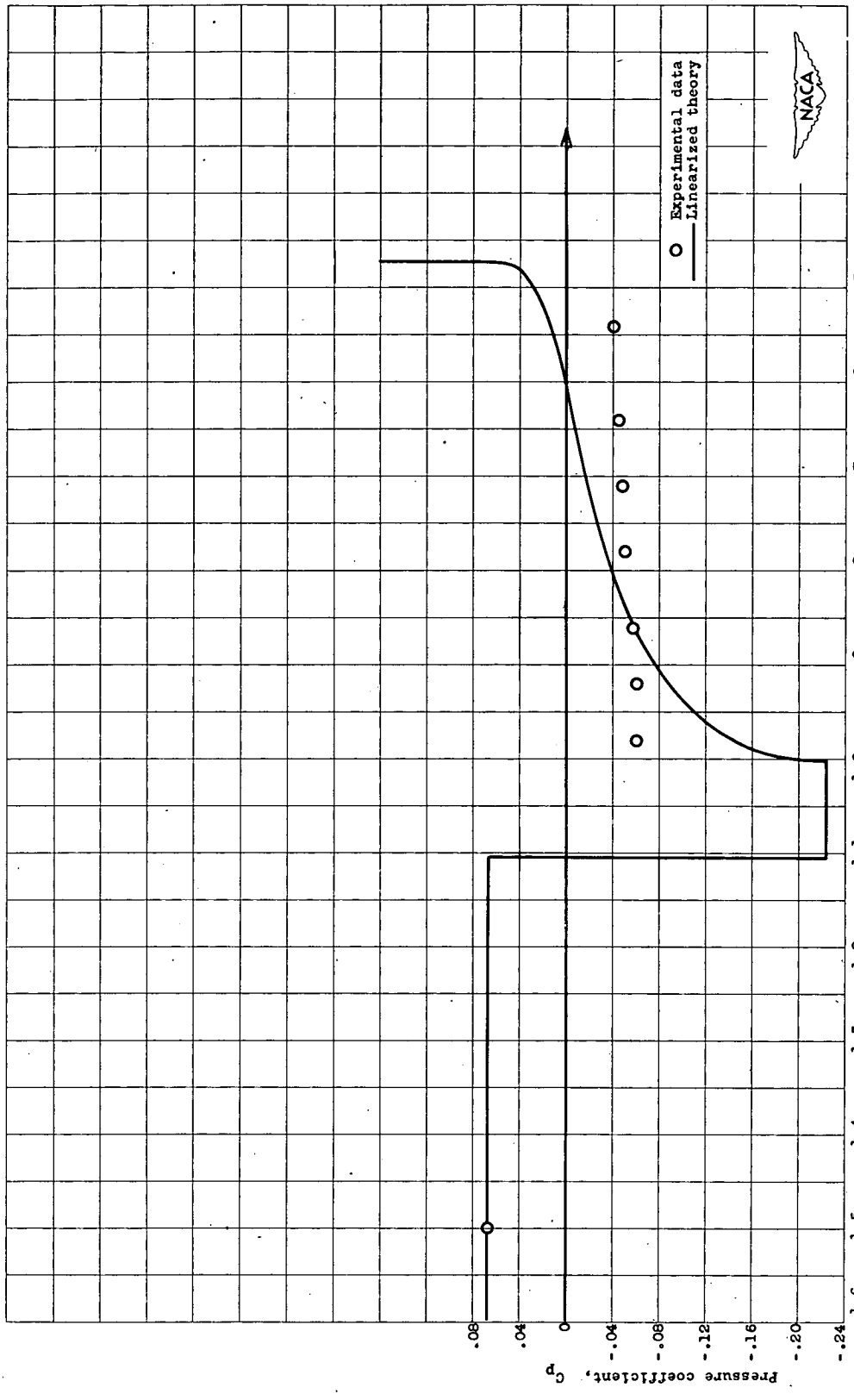

(a) Angle of attack, 0°.

Figure 4. - Spanwise variation of pressure coefficient.

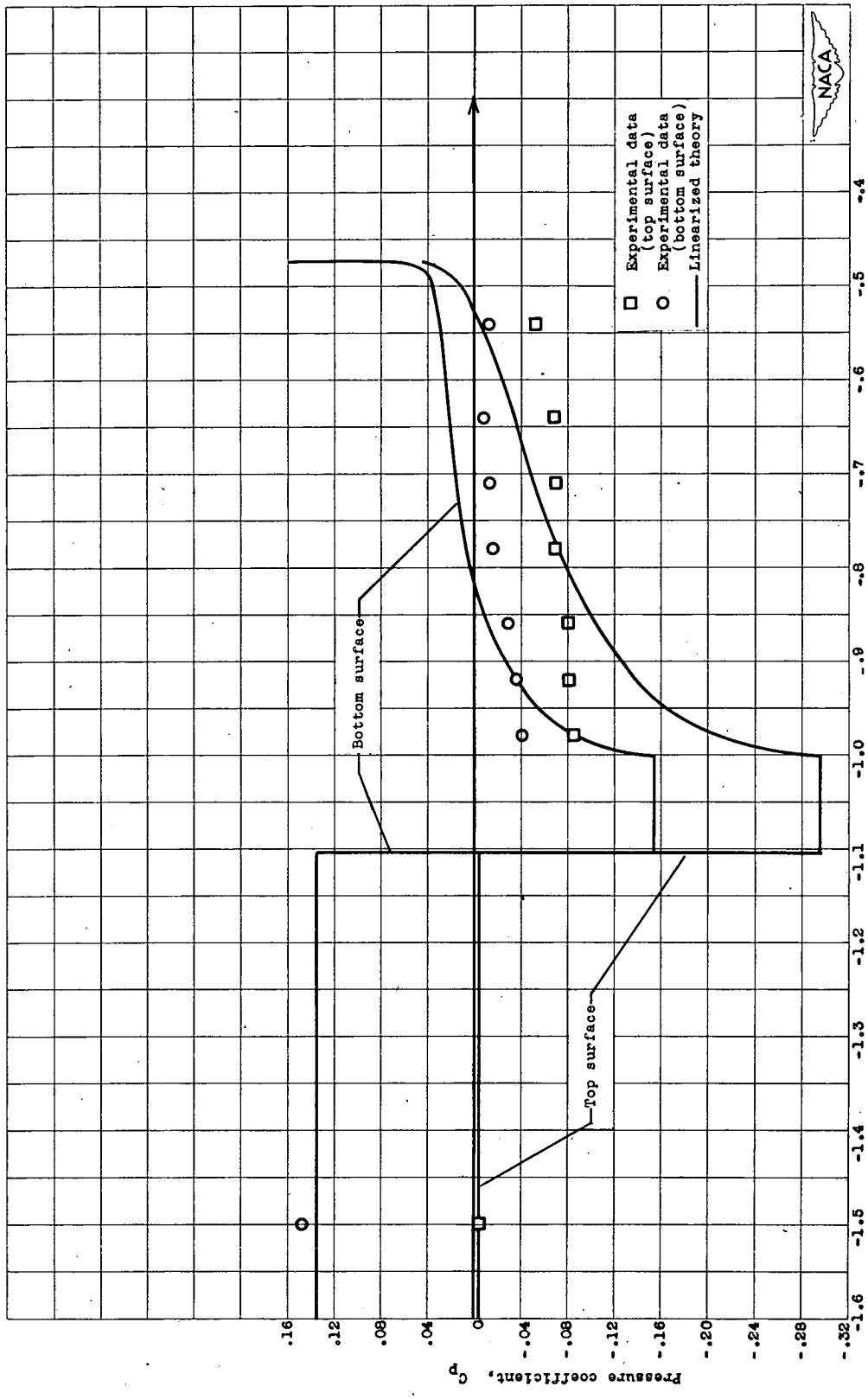

(b) Angle of attack, 3°.

Figure 4. - Continued. Spanwise variation of pressure coefficient.

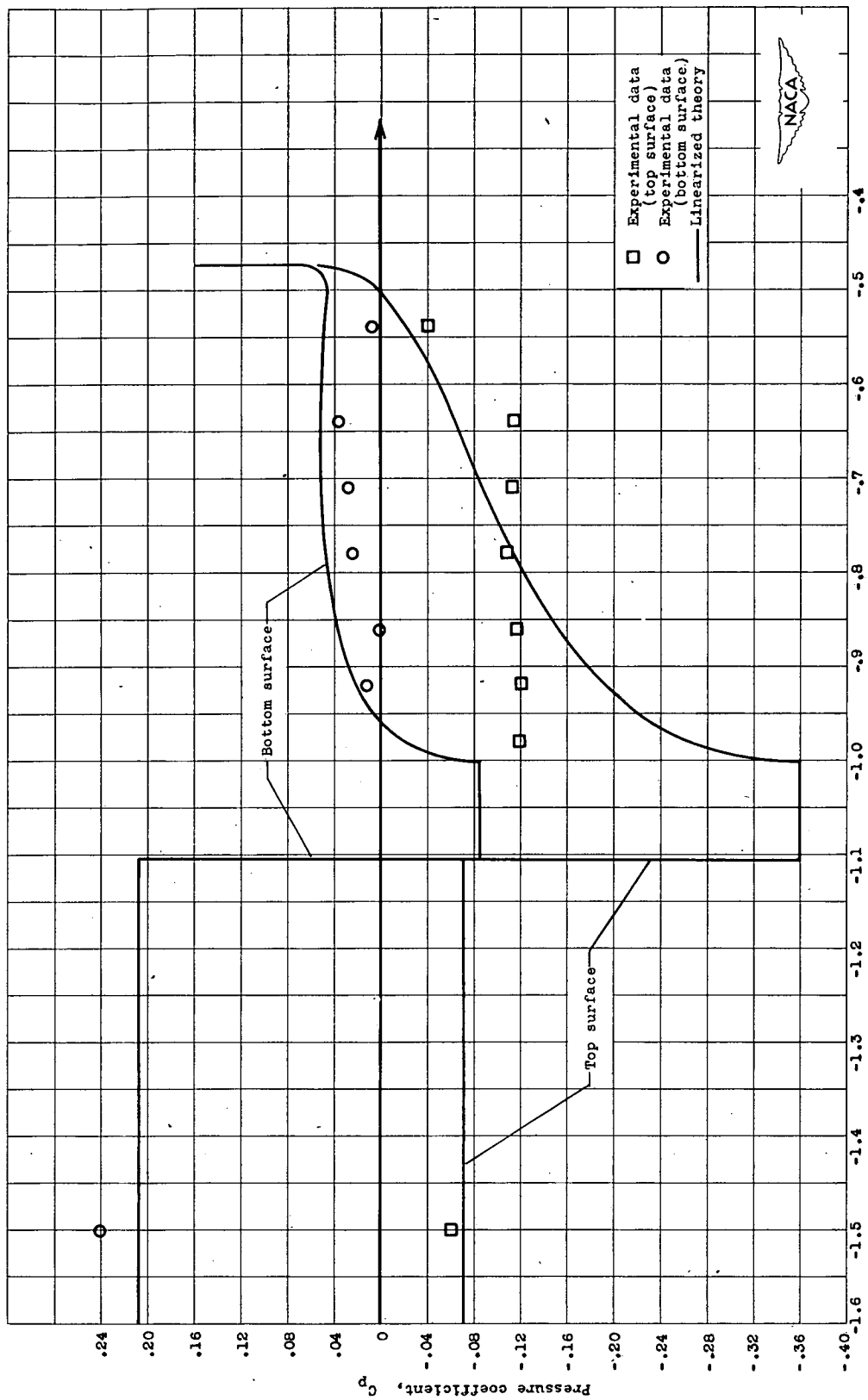

(c) Angle of attack, 6°.

Figure 4. - Continued. Spanwise variation of pressure coefficient.

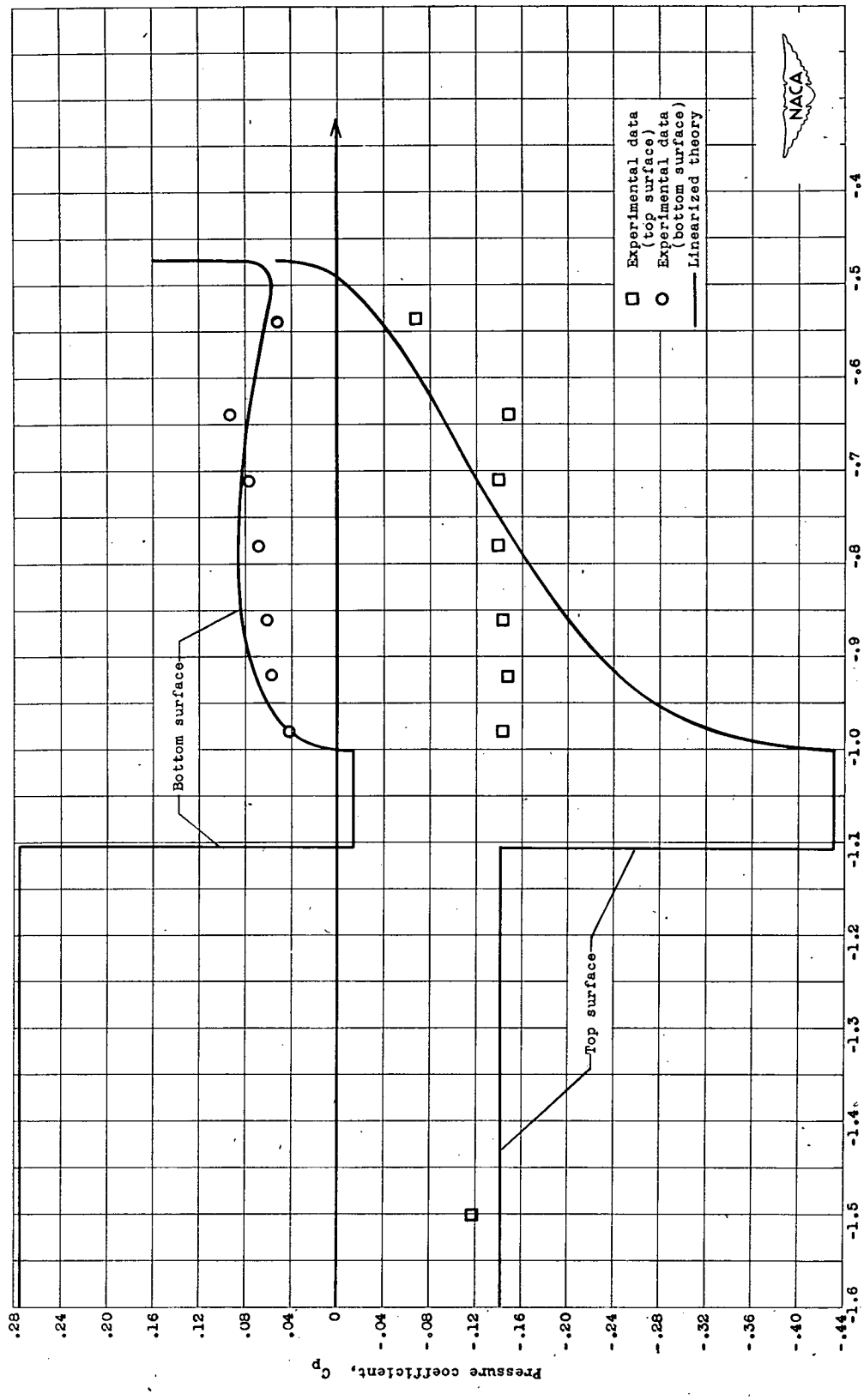

(d) Angle of attack, 9°.

Figure 4. - Concluded. Spanwise variation of pressure coefficient.